LEVENT AKYALÇIN

Anadolu University, Department of Chemical Engineering, Iki Eylul Campus, Eskişehir, Turkey

SCIENTIFIC PAPER

UDC 544.6:51

PERFORMANCE OPTIMIZATION OF AN AIR-BREATHING PEM FUEL CELL

Article Highlights
- The Taguchi method is useful to optimize the performance of an air-breathing PEM fuel cell
- The most effective parameter is determined to be the cathode catalyst loading
- The predicted and the obtained maximum power densities at a certain cell potential are very close
- The inclusion of environmental conditions may improve future optimization studies

Abstract

In this study, Taguchi's experimental design is used to determine the optimum component combination of a membrane electrode assembly and cathode current collector opening geometry to obtain maximum power density of an air-breathing polymer electrolyte membrane fuel cell at 0.5 V. An analysis of variance was conducted to figure out the optimum levels and significant differences of the effect of the combinations, followed by a performance measurement analysis. Experimental investigations of the effecting parameters enabled the determination of the optimum configuration of the MEA and cathode current collector opening geometry design parameters for maximum power density at a certain cell potential. Effective parameters which enable withdrawal of a maximum power output from an ABPEMFC at 0.5 V are, in order of effectiveness: the amount of platinum on the cathode, the thickness of the Nafion membrane, the cathode current collector opening geometry, and the amount of platinum on the anode. Optimum component combinations are: 0.45 mgPt cm^{-2} for the platinum loading on the cathode, Nafion 112 for membrane, a vertical cathode opening geometry and 1.78 mg cm^{-2} for the amount of platinum on the anode. For these component combinations, a 98.5 mW cm^{-2} power output was obtained from an ABPEMFC at 0.5 V cell voltage.

Keywords: air-breathing PEM fuel cell, performance optimization, Taguchi.

Air-breathing polymer electrolyte membrane fuel cells (ABPEMFCs) are promising power generating devices to be used either to charge batteries or to supply power directly to portable electronic equipment, such as smart phones, tablets and suchlike. The simplicity of their natural convection oxygen delivery, low weight, easy fuel charge and low operating temperatures make ABPEMFCs attractive for future portable power applications.

The performance of ABPEMFCs depends on both structural and environmental conditions. The catalyst loading on the electrodes, membrane thickness and cathode opening geometry for air delivery are the main structural factors affecting the performance of ABPEMFCs. Relative humidity and the temperature around the ABPEMFCs are other important parameters, which depend on environmental conditions.

Much research on ABPEMFCs has been published in the literature. Some of these researches have focused on the mathematical modeling of ABPEMFCs, either at a cell component level or at an overall system level. Other researches have mainly focused on experimental evaluation of parameters affecting the performance of ABPEMFCs, either at a cell component base or environmental conditions base.

However, evaluating the individual effects of the cell components and environmental conditions on fuel cell performance may fail to recognize the overall picture.

Fabian *et al.* investigated the performance of the air-breathing PEM (polymer electrolyte membrane) fuel cell in relation to ambient temperature and humidity in their study. They conclude that natural convection is predominant on mass and heat transfer at the cathode surface. Furthermore, they report that water content in the membrane electrode assembly plays a major role in the performance of the fuel cell. They found that 60 °C is a critical temperature for the transition of the membrane from being well-hydrated to dried out. It is also reported that critical transition temperature is almost independent from ambient conditions, but current density at the critical transition temperature is dependent on ambient temperature and humidity. As a result, they conclude that the optimal performance of the air-breathing PEM fuel cell has a complex function of ambient and load conditions as well as of cell design [1].

Williamson *et al.* evaluated experimentally the impact of cell temperature on both open-cathode PEM fuel cells and closed-cathode PEM fuel cells by means of polarization scans and impedance spectroscopy. They chose PEM fuel cells having three different active surface areas for testing at different cell temperatures. The results of their studies show that a 5 cm^2 open-cathode PEM fuel cell reaches its peak power output at 40 °C. They conclude that an open-cathode PEM fuel cell is practicable for low power devices at a certain temperature [2].

Jeong *et al.* investigated the effects of cathode structure and water transport in air-breathing PEM fuel cells. They managed the cathode structure into two parts, namely the catalyst layer and the gas diffusion layer. They kept the anode catalyst loading constant at 0.4 mgPt cm^{-2}, while the cathode catalyst loading was changed from 0.3 to 1.6 mg Pt cm^{-2}. They report that when the effect of the catalyst loading was tested, the relative humidity was 30 and 60%. On the other hand, the effect of a gas diffusion layer was examined by changing the thickness of the gas diffusion layer (GDL) from 100 to 370 μm. They report that the best results are achieved by a MEA having a 0.6 mg Pt cm^{-2} cathode catalyst loading, and a 280 μm GDL thickness having 5-10% PTFE content. Furthermore, they interpret water transport in terms of net water drag coefficient [3].

Bussayajarn *et al.* aimed at designing a light weight planar air-breathing PEM fuel cell stack to supply energy for portable devices. They investigated different cathode opening designs having the same opening ratios to improve the stack performance and stability of the air-breathing PEM fuel cell. They report that the best performance and the highest limiting current density are obtained using a circular opening design. They conclude that rib distance and hydraulic diameter have significant effects on cell performance, and that both have to be minimized to increase mass transport and oxygen distribution [4].

Kim *et al.* used thin flexible printed circuit boards as a current collector to reduce the volume of the air-breathing PEM fuel cell stack. They also investigated the effects of the geometry of the cathode openings on the performance of the stack. As a result, they found that a rectangular cathode opening with a 65% opening ratio exhibited the best performance and voltage stability [5].

Ferreira-Aparicio and Chaparro investigated the influence of a gas diffusion cathode structure on the performance of an air-breathing PEM fuel cell. They manipulated both catalytic layer thicknesses using different amounts of platinum content on carbon and on the cathode gas diffusion layer using different gas diffusion media. They conclude that woven gas diffusion substrates show better performance at higher current densities than unwoven substrates, because the macro-porous structure expels water from the reaction media and a very high catalyst content allows a reduction in the catalytic layer thickness, contributing to Pt utilization [6].

The design of experiments, known as factorial design, is a technique defining and investigating all possible conditions in an experiment, considering multiple factors. The full factorial and fractional factorial designs come under the design of experiments. Full factorial experiments investigate all-possible combinations of factors and their levels. On the other hand, fractional factorial experiments investigate the fraction of all possible combinations. This approach saves considerable time and money, but it requires careful mathematical treatment, in both the design of the experiments and in the evaluation of the results. Furthermore, two experimenters may design different sets of fractional factorial experiments. Taguchi simplified and standardized fractional factorial designs, yielding similar data and similar conclusions for the same design of experiments prepared by different experimenters. Consequently, Taguchi overcame the limitations of factorial and fractional factorial experiments. Orthogonal arrays (OA) are used in Taguchi's designs of experiments. These are specially constructed tables to make the design of experiments easier and consistent [7,8].

An experimental matrix consisting of a set of experiments allows for a change in the setting of the parameters under study in an experiment. The data obtained from the experimental matrix are analyzed together to determine the effects of the various parameters. Conducting experiments using special matrices, called orthogonal arrays, allows for an estimation of the effects of several parameters to be determined efficiently and is an important technique in robust design. Each column in the orthogonal array corresponds to a factor affecting the experiment, and the levels of the factors are set in the column. All combinations of the levels of the factor in any pair of columns occur, and they occur in an equal number of times. This is called the balancing property and it implies orthogonality. Furthermore, each row represents a trial condition with factor levels indicated by the numbers in the row. The usage of orthogonal arrays makes the design of experiments easy and consistent [7,8].

The Taguchi method is a design of experiment which can be applied to any situation that depends on many influencing factors, like variables, inputs, parameters, and so on. The main advantage of the Taguchi method over other designs of experiments is that the factors can be investigated either as controlling or non-controlling. When we consider ABPEMFCs, there are controllable factors like the MEA combination and cathode current collector opening geometry and non-controllable factors like the humidity and temperature of the working environment. In addition, the experimentation costs can be minimized while keeping the mean response on target. For these reasons, the Taguchi method allows for the design of robust ABPEMFC architecture for different operations and different environmental conditions [9].

In this study, Taguchi's experimental design is used to determine the optimum component combination of a membrane electrode assembly (MEA) and cathode current collector opening geometry to obtain maximum power density of an air-breathing polymer electrolyte membrane (PEM) fuel cell (ABPEMFC) at 0.5 V. An analysis of variance was conducted to figure out the optimum levels and significant differences of the effect of the combinations, followed by a performance measurement analysis.

MATERIAL AND METHODS

SGL Carbon 25BC was used as the gas diffusion layer (GDL) in each experiment. The substrate was cut to dimensions of 10 cm×10 cm and weighed. Catalyst ink was prepared by mixing 60% Pt on carbon black (Alfa Aesar HiSPEC 9000), 5 wt.% Nafion solution (Ion Power, LQ-1005), isopropanol and deionized water (18.2 MΩ) ultrasonically for 6 min.

The catalyst inks were ultrasonically sprayed onto the GDLs at different catalyst loadings of 0.45, 1.35 and 1.78 mg Pt cm^{-2}, using a Sono-Tek Exacta-coat ultrasonic spray instrument operating at 48 kHz. The catalyst inks (25 ml) were first filled into a sonicated (60 kHz) syringe prior to nozzle atomization (Accumist) and sprayed at a flow rate up to 2.6 ml min^{-1} by means of a syringe pump. The GDLs were placed onto a combined heat/vacuum plate during the spraying, with the plate heated up to 40 °C. The spraying process was done several times (up to 6 in total) to reach desired loading. The produced electrodes were then dried at 80 °C for 12 h. The amount of catalyst loaded onto the GDLs was calculated by the change in weight of the GDL. The electrodes were die cut into small pieces at dimensions of 2 cm×2.5 cm and kept in separate zipped plastic bags from their catalyst loadings. These electrodes were selected randomly from the zipped plastic bag for use in the experiments.

Nafion 112, 1135 and 115 were used as polymer electrolytes in the experiments. The die-cut membranes were immersed in deionized water for 15 min at 90 °C and then immersed in a 5% H$_2$O$_2$ solution for 60 min to remove organic impurities. Before these membranes were immersed in a 0.5 M H$_2$SO$_4$ solution for 30 min at 90 °C to remove inorganic impurities, they had been rinsed in deionized water for 15 min at 90 °C. The step to remove inorganic impurities was repeated using fresh solution. After this, the membranes were rinsed in deionized water for 15 min at 90 °C, with this step being repeated three further times. At the end of the cleaning procedure, the clean membranes were kept in deionized water up until their use in the experiments.

Both the anode and the cathode current collector plates had active areas of 5 cm^2 manufactured from Type 316 stainless steel. The anode current collector, shown in Figure 1a, has serpentine gas flow channels of 1 mm width and 1 mm depth, with ribs of 1 mm width. The thickness of the anode current collector is 16 mm. The gas flow channels are placed in the center of both the anode and the cathode current collectors. The thickness of the cathode current collector plates is 2 mm. The cathode openings widths are 2 mm for the vertical openings shown in Figure 1b, and the oblique openings are shown in Figure 1d. The diameter of the circular opening, shown in Figure 1c, is 2 mm. The surfaces of the current collectors contacting with the GDEs were smoothed mechanic-

ally. The area ratios of the vertical, oblique and circular openings to the total planar surface area of 5 cm^2, are 0.72, 0.69 and 0.50, respectively.
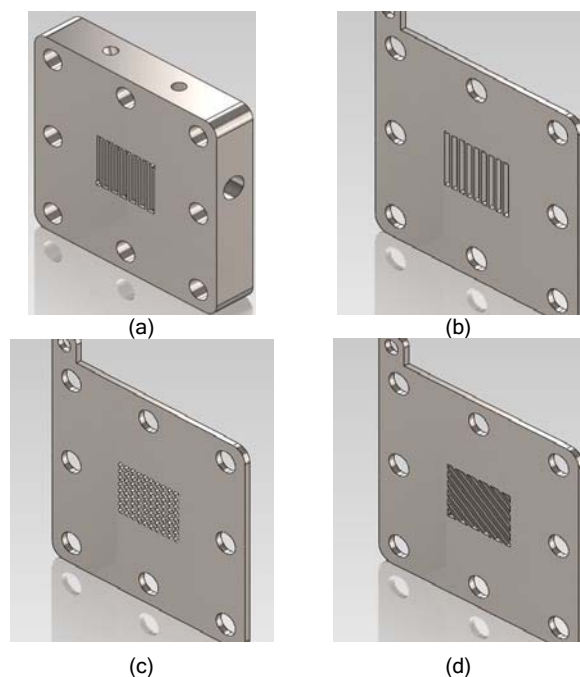

(a)   (b)

(c)   (d)

Figure 1. a) Anode current collector; b) cathode current collector with vertical cathode-opening geometry; c) cathode current collector with circular cathode-opening geometry; d) cathode current collector with oblique cathode-opening geometry.

The experimental setup used in this study is shown in Figure 2. In each experiment, 99.999% pure hydrogen with a flow rate 10 times its theoretical amount was fed to the anode of the fuel cell. This was done to avoid insufficient reactant. The cathode side was open to laboratory atmosphere and the location of the fuel cell was protected from the forced convection of air to the cathode side. The reactant gases were not humidified externally. The room temperature was kept at 20 °C by air-conditioning. The tempera-
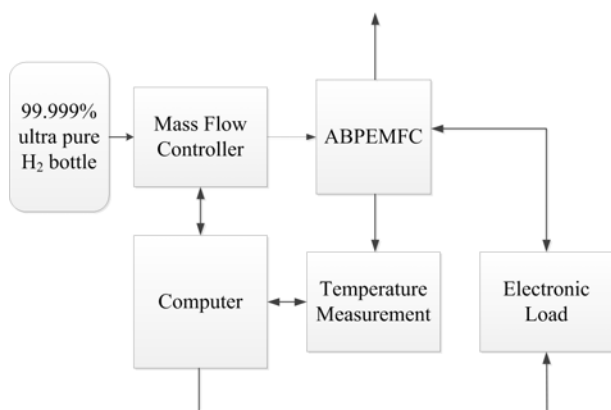

Figure 2. A schematic drawing of the experimental apparatus.

ture of the fuel cell was monitored and recorded throughout the experiments by Agilent 34970A data acquisition and a switching unit with the calibrated Type-K thermocouple. Pure hydrogen (99.999%) gas was delivered from a pressurized gas bottle. A Brooks mass flow controller controlled the volumetric flow rate of the hydrogen gas. The pressure of the delivered hydrogen was kept at 0.1 bar throughout the experiments. All of the polarization curves throughout the experiments were obtained by a Solartron 1260A//1287A full electrochemical system. The experiments were conducted potentio-dynamically. The cell potential was decreased with 1 mV s^{-1} from an open circuit cell voltage (OCV) to 0.2 V and increased at the same rate from 0.2 V to OCV in each experiment. This scanning procedure was repeated ten times for each fuel cell configuration. An overall average of the ten scans was evaluated as the characteristic polarization values of the corresponding fuel cell configuration.

Experimental parameters and their levels given in Table 1 are determined in the light of the literature and preliminary testing. The L_9 (3^4) OA, given in Table 2, was accepted as the most correct method to determine the experimental plan for four parameters (A, B, C, D) each of three levels (1, 2, 3). The performance of the ABPEMFC may be affected by controllable or uncontrollable (noise sources) factors. In order to minimize the effects of uncontrollable factors, each experiment was repeated three times with the same combination of parameters. The order of each experiment given in Table 2 was randomized to avoid noise sources, which could occur throughout the experimentation and affect results negatively, at each repetition.

Table 1. Experimental parameters and their levels

Parameter	Level		
	1	2	3
A. Anode Pt loading, mg Pt cm^{-2}	0.45	1.35	1.78
B. Cathode Pt loading, mg Pt cm^{-2}	0.45	1.35	1.78
C. Nafion membrane	112	1135	115
D. Cathode current collector opening geometry	Vertical	Circular	Oblique

A signal is the desired effect in which the performance characteristics of a system under testing give response to a parameter in the experiment design. External factors, which are uncontrollable parameters and affect the outcome, are called noise factors and their effects are termed noise. It is expected to have the highest possible signal-to-noise ratio in Taguchi's method. The higher S/N corresponds

Table 2. Experimental plan

No. of experiment	A	B	C	D
1	1	1	1	1
2	1	2	2	2
3	1	3	3	3
4	2	1	2	3
5	2	2	3	1
6	2	3	1	2
7	3	1	3	2
8	3	2	1	3
9	3	3	2	1

to the lower random effects of the noise factors. It can be concluded that the highest S/N results in the optimum quality with minimum variance. The quality concept can be considered in three categories: "smaller-the-better", "nominal-the-best" and "larger--the-better". In this study, the quality characteristic was chosen as "larger-the-better" to maximize cell performance [7,8]. Eq. (1) calculates the S/N:

$$S/N = -10 \log MSD \tag{1}$$

The mean squared deviation (*MSD*) is defined, as in Eq. (2), for the "larger-the-better" quality characteristic:

$$MSD = (1/Y_1^2 + 1/Y_2^2 + 1/Y_3^2 + \cdots)/n \tag{2}$$

When the optimum, which maximizes the power density, is not one of the trial runs in the experimental plan, it is necessary to run a conformation test(s). The direct proof of the approach of Taguchi's method is the conformation test. The average of the results from the conformation tests should be consistent with the optimum performance assessed by the analysis. An additive model can be used for this aim. An additive model is the sum of the overall mean μ for the experiment region; the deviation from μ is caused by setting the factor at a certain level and error. The error implied is the error of the additive approximation plus the error in the repeatability of measurement for a given experiment [7,8]. Eq. (3) gives the additive model:

$$Y_i = \mu + X_i + e_i \tag{3}$$

Since Eq. (3) is the point estimation, which is calculated using experimental data in order to determine whether the additive model is adequate or not, confidence limits for the prediction error must be evaluated. The prediction error is the difference between the observed Y_i and the predicted Y_i. The confidence limits for the prediction error, *Se*, is:

$$Se = \pm 2 \sqrt{\frac{1}{n_0}\sigma_e^2 + \frac{1}{n_r}\sigma_e^2} \tag{4}$$

$$\sigma_e^2 = \frac{\text{Summ of squares due to error}}{\text{Degrees of freedom for error}} \tag{5}$$

$$\frac{1}{n_0} = \frac{1}{n} + (\frac{1}{n_{A_i}} - \frac{1}{n}) + (\frac{1}{n_{B_i}} - \frac{1}{n}) + (\frac{1}{n_{C_i}} - \frac{1}{n}) + \cdots \tag{6}$$

If the prediction error is outside these limits, it is possible that the additive model is not acceptable. Otherwise, it may be considered that the additive model is beneficial [7,8].

After determining the optimum conditions and predicting the response under these conditions, a confirmation experiment can be conducted with optimum parameter settings, and the results obtained from the experiment can be compared with the prediction. If the observed and predicted values are close, then it can be concluded that the additive model is sufficient to describe the dependence of Y_i on the various parameters. Otherwise, it implies that the additive model is inadequate and the interactions are important [7,8].

In this study, L_9 (3^4) OA was selected as the experimental plan given in Table 2. Each column in Table 2 corresponds to a parameter and cells under each column corresponds to the levels of the related parameter. The order of experiments was randomized in order to avoid noise sources which were not predicted and which could occur during an experiment and thereby affect results.

RESULTS AND DISCUSSION

Polarization and power density curves

The experiments were performed randomly by means of the experimental set-up. Polarization scans were performed potentiodynamically and repeated ten times under the same operating conditions for each MEA and cathode current collector geometry combination. Green run polarization scans were performed by each cell combination until it reaches its maximum and stable polarization scan values before the ten times polarization scans. Experiments were repeated three times for every MEA and cathode current collector opening geometry combination at different times. A power density obtained at 0.5 V was used in the statistical analysis for each run. Polarization curves obtained from each experiment are presented in Figure 3, as cell potential versus the average of the
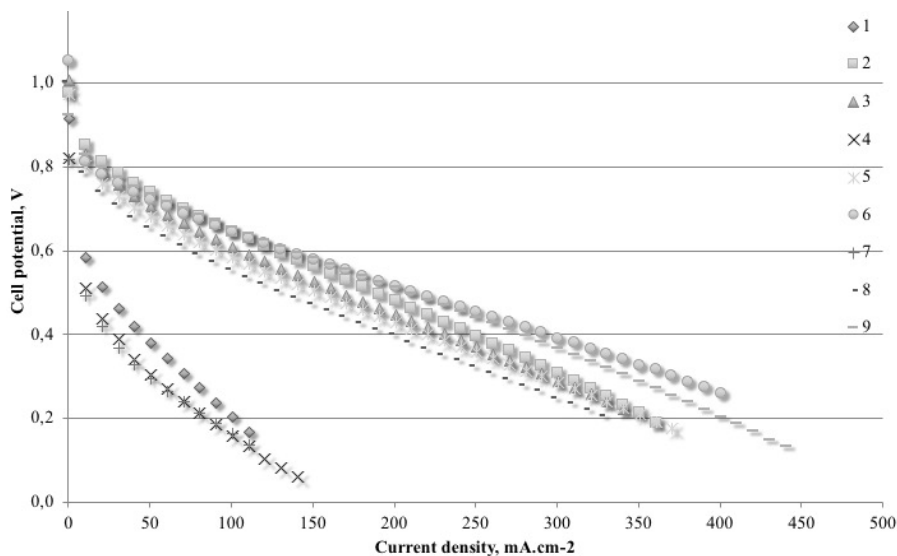
Figure 3. Polarization curves obtained from each experiment.

current densities of ten scans. Power density curves were determined from the cell potential and the average of current densities and are presented in Figure 4, as power density versus current density. The power densities at 0.5 V obtained from the trials are tabulated in Table 3.

Statistical analysis

Since the Taguchi method replaces the full factorial experiments with fractional factorial experiments, based particularly on OAs, it is necessary to analyze the confidence. For this reason, an analysis of variance (ANOVA) is used to analyze the confidence. This technique determines the variability of the data and confidence is measured from the variance. The

Table 3. The power densities at 0.5 V (mW cm^{-2}) obtained from the trials

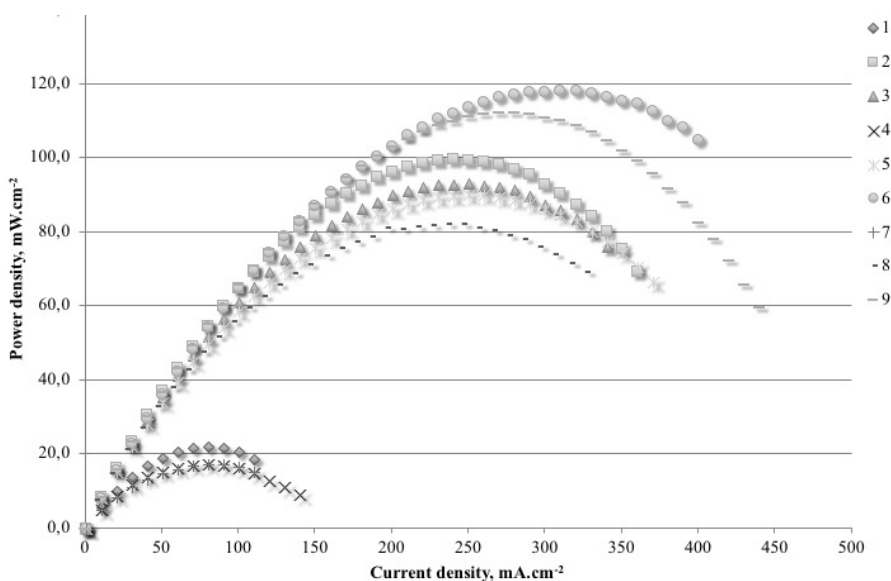| Experiment No.	Trial			
	1st	2nd	3rd	Average
1	5.37	10.96	11.34	9.22
2	84.25	94.32	90.41	89.66
3	71.46	84.11	83.45	79.67
4	6.31	6.04	5.24	5.86
5	63.96	76.99	69.99	70.31
6	111.28	106.85	103.49	107.21
7	2.92	4.78	3.05	3.58
8	79.67	76.97	67.58	74.74
9	96.62	102.31	105.65	101.53

Figure 4. The power density curves determined from the cell potential and the average of the current densities.

analysis provides the variance of controllable and uncontrollable factors. By recognizing the source and magnitude of variance, parameters which make the system robust, can be predicted [7,8].

Minitab17® software was used to analyze the collected data. An ANOVA was performed in order to observe effective MEA and cathode current collector opening geometry parameters in obtaining the maximum power density of the ABPEMFC at 0.5 V. The F-test is a powerful tool used to observe which parameters have a significant effect in obtaining the maximum power density at certain cell potentials.

Variance ratio, denoted by F, is the ratio of the mean square due to a factor and the error mean square. A large value of F implies that the effect of that factor is large compared to the error variance. Furthermore, the larger the value of F, the more important the factor, which influences the maximum power density [7-9].

Signal-to-noise ratio and ANOVA analyses are complementary tools for prediction of the optimal combination of parameters. The ANOVA results relating to the experiments are given in Table 4 [10].

Table 4. The results of the variance analysis for the experiments

Source	DF	SS	MS	F	p
A	2	12,5	6.2	0.27	0.766
B	2	40771.9	20385.9	882.32	0.000
C	2	1112.9	556.5	24.08	0.000
D	2	807.3	403.6	17.47	0.000
Error	18	415.9	23.1	-	-
Total	26	43120.4	-	-	-

The "larger-the-better" performance characteristic, shown in Eq. (1), is used in order to obtain the maximum power density of an ABPEMFC at 0.5 V. The order of graphs in Figure 5, prepared for the experiments, is according to the parameters given in Table 1. The optimal level of a parameter in obtaining the maximum power density at certain cell voltages is the level with the highest S/N value calculated by Eq. (1).

The variation of S/N with cathode current collector opening geometry is given in Figure 5. In this figure, the third data point corresponds to oblique geometry of the cathode current collector opening. The experiments for which the D level (column D) is 3 are experiments numbers 3, 4 and 8. The performance characteristics value of the third data point is the average of those obtained from experiments 3, 4 and 8. All the data points given in Figure 5 are determined using the same approach. The numerical value of the data point, which has a maximum S/N ratio, maximizes the power density of an ABPEMFC. These data points and their numerical values are A1 (0.45 mg Pt cm^{-2}), B3 (1.78 mg Pt cm^{-2}), C1 (Nafion 112) and D1 (vertical cathode opening geometry). It can be seen that the A1, B3, C1 and D1 combination does not take place in the experimental plan. However, it is possible to predict the power density for such a combination from the experimental results using Eq. (3). Verification experiments were conducted three times and both the average of the observed results from the verification experiments and the predicted value for the same combination are summarized in Table 5. Under these conditions, the average current density was measured as 197 mA cm^{-2} at 0.5 V cell
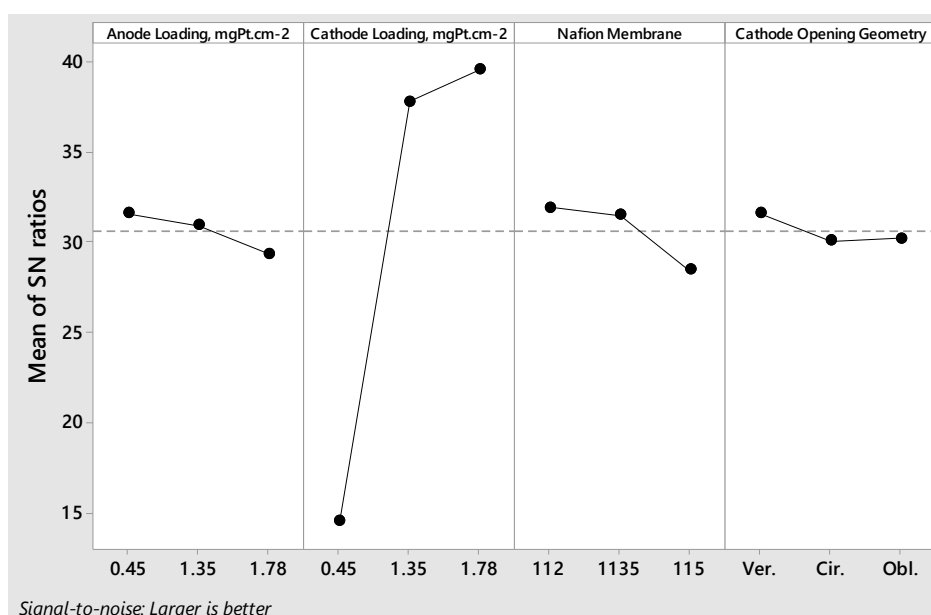

Signal-to-noise: Larger is better

Figure 5. The mean effects plot for S/N.

Table 5. Optimum MEA and cathode current collector opening geometry, observed and predicted maximum power densities at 0.5 V cell potential

Parameter	Value	Level
Anode Pt loading, mgPt cm^{-2}	0.45 mg Pt cm^{-2}	1
Cathode Pt loading, mgPt cm^{-2}	1.78 mg Pt cm^{-2}	3
Nafion membrane	Nafion 112	1
Cathode current collector opening geometry	Vertical	1
Predicted maximum power density at 0.5 V cell potential (mW cm^{-2}) for 95% of confidence limit	99.14	-
Observed maximum power density at 0.5 V cell potential (mW cm^{-2})	98.50	-
Confidence limits of prediction for maximum power density at 0.5 V cell potential (mW cm^{-2})	84.81-113.47	-

potential, and average power density was determined as 98.5 mW cm^{-2}.

It can be seen that the average power density obtained from the verification experiment is within the calculated confidence limits from Eqs. (4)-(6). It can be concluded from this case that the predicted and experimental results match each other and also that the interaction between parameters is negligible. Furthermore, it can be deduced that the additive model is adequate to describe the dependence of the performance of this ABPEMFC on various parameters.

On the other hand, the higher values of experiments nos. 6 and 9 than the verification experiment are recognizable. It can be seen that the suggested combination and the combination of experiment No. 6 have common levels of parameters; $B3$ and $C1$. Furthermore, the results getting from the experiment No. 6 is better than the experiment No. 9 because of the thinner membrane, $C1$, used in the experiment. This result is supported with the F values calculated in ANOVA analysis, which gives the most effective parameters as B (cathode platinum loading) and C (membrane), respectively. For these reasons, the obtained results for the suggested configuration and experiments Nos. 6 and 9 are compatible and all in the 95% confidence interval.

Contributions of cell components

Platinum on carbon black was used as catalyst on both anode and cathode electrodes. Hydrogen oxidation reaction (HOR) is extremely fast on Pt so that the Pt loading can be reduced on the anode electrode. Furthermore, if the catalyst loading increases on the anode electrode, it creates resistance against the mass flow of hydrogen and effects the cell performance negatively. This behavior can be seen in Figure 5 clearly.

On the other hand, the sluggish reaction kinetics of oxygen reduction reaction (ORR) is six or more orders of magnitude slower than the anode HOR and it can be improved with the increasing catalyst loading

on cathode electrode. This case can also be seen in Figure 5. Beyond that, the overall performance of ABPEMFC is highly dependent on the cathode electrode performance, which is also approved with ANOVA in this study.

Ferreira *et al.* reported that the decreasing membrane thickness results into considerably higher performances, due to a decrease in ohmic resistance. They also reported that a rapid recovery from dehydration is observed when a thinner membrane is employed at low air humidity operation [11]. That conclusion is also observed and supported with signal-to-noise ratios and ANOVA in this study.

The area ratios of the vertical, oblique and circular openings to the total planar surface area of 5 cm^2, are 0.72, 0.69 and 0.50, respectively. The vertical opening has the biggest opening ratio, which allows the higher air intake to cathode electrode, resulting in better contribution to the cell performance. Moreover, even if the opening ratios are close to each other, signal-to-noise ratios of the results of the designed experiments response precisely to small changes.

CONCLUSION

The optimization of the structural combination of an MEA and cathode current collector opening geometry in obtaining maximum power density of an ABPEMFC is important for understanding the synergetic effects of the components on system performance.

In this study, the Taguchi method was employed to determine the optimum parameters in obtaining the maximum power density of an ABPEMFC.

The parameters for maximum power density from an ABPEMFC at 0.5 V are in order of effectiveness: the amount of platinum on the cathode, the thickness of the Nafion membrane, cathode current collector opening geometry, and the amount of platinum on the anode.

The optimum conditions within the selected parameter values are: 0.45 mg Pt cm^{-2} for the amount of platinum on the cathode, Nafion 112 for the membrane, vertical cathode opening geometry, and 1.78 mg Pt cm^{-2} of platinum on the anode. Under these conditions, a maximum power density of 98.5 mW cm^{-2} was obtained from the verification experiment.

The predicted and the obtained maximum power densities at a 0.5 V cell potential are extremely close. It may be concluded that the additive model is adequate for describing its dependency on obtaining maximum power density at various parameters.

Acknowledgement

Nomenclature

e_i	Random error in the ith experiment
n	number of rows in the matrix experiment
$n_{Ai}, n_{Bi}, n_{Ci}...$	Replication numbers for parameter levels $A_i, B_i, C_i, ...$
n_r	Number of repetitions for the verification experiment
n_0	Equivalent sample size
Se	two-standard-deviation confidence limit
S/N	Performance characteristics for "larger-the-better"
X_i	Fixed effect of the parameter level combination used in the ith experiment
Y_i	Performance value of the ith experiment

Greek letters

μ	Overall mean of performance value
σ_e	Error variance

REFERENCES

[1] T. Fabian, J.D. Posner, R. O'Hayre, S.W. Cha, J.K. Eaton, F.B. Prinz, J.G. Santiago, J. Power Sources 161 (2006) 168-182

[2] Z. Williamson, D. Kim, D.K. Chun, T. Lee, C. Squibb, Appl. Therm. Eng. 31 (2011) 3761-3767

[3] S.U. Jeong, E.A. Cho, H.J. Kim, T.H. Lim, I.H. Oh, S.H. Kim, J. Power Sources 159 (2006) 1089-1094

[4] N. Bussayajarn, H. Ming, K.K. Hoong, W.Y.M. Stephen, C.S. Hwa, Int. J. Hydrogen Energy 34 (2009) 7761--7767

[5] S.H. Kim, H.Y. Cha, C.M. Miesse, J.H. Jang, Y.S. Oh, S.W. Cha, Int. J. Hydrogen Energy 34 (2009) 459-466

[6] P. Ferreira-Aparicio, A.M. Chaparro, Int. J. Hydrogen Energy 39 (2014) 3997-4004

[7] M.S. Phadke, Quality engineering using robust design, Prentice Hall, Englewood Cliffs, NJ, 1989

[8] R.K. Roy, A primer on the Taguchi method, Society of Manufacturing Engineers, Dearborn, MI, 1990

[9] R.K. Roy, Design of experiments using the Taguchi approach : 16 steps to product and process improvement, Wiley, New York, 2001

[10] S. Kaytakoglu, L. Akyalcin, Int. J. Hydrogen Energy 32 (2007) 4418-4423

[11] R.B. Ferreira, D.S. Falcao, V.B. Oliveira, A. Pinto, Electrochim. Acta 224 (2017) 337-345.

LEVENT AKYALÇIN

Anadolu University, Department of
Chemical Engineering, Iki Eylul
Campus, Eskişehir, Turkey

NAUČNI RAD

OPTIMIZACIJA PERFORMANSI PEM GORIVNE ĆELIJE SA SLOBODNIM DOPREMANJEM VAZDUHA

U ovoj studiji, eksperimentalni plan Taguchi se koristi za određivanje optimalne kombinacije komponenti sklopa membrana-elektrode i geometrije katodnog strujnog kolektora da bi se dobila maksimalna gustina snage PEM gorivne ćelije sa slobodnim dopremanjem vazduha pri 0.5 V. Sprovedena je analiza varijanse kako bi se odredili optimalni nivoi i značajne razlike u efektu kombinacija, nakon čega je sledila analiza merenja performansi. Eksperimentalnim istraživanjima efektivnih parametara omogućeno je određivanje optimalne konfiguracije parametara geometrijskog oblika MEA i katodnog strujnog kolektora za maksimalnu gustinu snage na određenom potencijalu ćelije. Efektivni parametri koji omogućavaju povlačenje maksimalne izlazne snage iz ABPEMFC-a na 0.5 V su, po redu, efektivnost, količina platine na katodi, debljina Nafionove membrane, geometrija katodnog strujnog kolektora i količina platine na anodi. Optimalne kombinacije komponenata su 0,45 mg Pt cm^{-2} za platinsko opterećenje na katodi, Nafion 112 za membranu, vertikalna geometrija katodnog otvaranja i 1,78 mg cm^{-2} za količinu platine na anodi. Za ove kombinacije komponenata, izlazna snaga od 98.5 mW cm^{-2} dobijena je iz ABPEMFC-a na naponu ćelija od 0.5 V.

Ključne reči: PEM ćelija sa slobodnim dopremanjem vazduha, optimizacija performansi, Taguchi.